Effect of SAPs and polypropylene fibres on the freeze-thaw resistance of low carbon roller compacted concrete pavement

Vahid Afroughsabet[1*], and *Abir* Al-Tabbaa[1]

[1]Department of Engineering, University of Cambridge, Trumpington Street, Cambridge CB2 1PZ, UK

Abstract. Most concrete currently used in pavement is based on Portland cement (PC), being responsible for 8-10% of total CO_2 emission. Moreover, external pavements are subjected to exposure classes XF4 and XD3 which are related to corrosion and freeze-thaw. Freeze-thaw resistance is an important durability property of concrete, especially for concrete pavements that are subjected to the de-icing salts. This study was designed to explore the freeze-thaw resistance and mass scaling resistance of low carbon Roller Compacted Concrete (RCC) in the presence of water and de-icing salts. Four different RCC mixes were used with a water/binder ratio of 0.45. PC was replaced with 80% ground granulated blast-furnace slag (GGBS) in all mixes to develop low carbon concrete and move towards a more sustainable cementitious composite. To assess the effectiveness of smart engineered additives, superabsorbent polymers (SAPs) were used at 0.3% by weight of total binder, and Polypropylene (PP) fibre with 12-mm length at fibre volume fractions of 0.3% for the mitigation of freeze-thaw damage. The compressive strength, freeze-thaw resistance, and mass scaling resistance of concrete specimens were evaluated. The results indicate that both additives improved the compressive strength and freeze-thaw resistance of concrete with and without de-icing salts. The inclusion of PP fibre was more effective compared to the addition of SAPs to mitigate the extent of internal structural damage and mass scaling of self-healing concrete mixes with respect to the reference concrete after 56 freeze-thaw cycles.

Keywords: Concrete pavement; Freeze-thaw resistance; De-icing salts, Superabsorbent polymers (SAPs); Polypropylene Fibres; GGBS.

1 Introduction

Concrete is a key construction material for different infrastructure assets such as bridges, roads, and buildings due to the several promising benefits it presents compared to other construction materials such as its general availability, low cost, formability, and broad applicability [1]. Rigid concrete pavements are broadly employed in the construction of long-lasting and durable roads [2]. Roller compacted concrete (RCC) is a special type of rigid concrete pavement that has gained an increased attention due to its relatively efficient and cost-effective process and was recently added to the UK specification [3]. Like other infrastructure assets, most concrete currently used in pavement is based on Portland cement (PC) that its production results in a high volume of CO_2 emission into the environment. UK alone cement consumption is about 11.7 Mt per year that results in 1.5% greenhouse gas emissions, while PC production accounts for about 8-10% of total CO_2 emissions [4]. To mitigate the harmful impact of cement utilisation and maintain progress towards CO_2 reduction, the current approach is to develop low carbon concrete by partially replacing the PC with supplementary cementitious materials (SCMs) such as fly ash, silica fume, natural pozzolans, and ground granulated blast-furnace slag (GGBS) [5]. It is well documented that the addition of SCMs, particularly at low content can improve the durability of concrete materials such as chloride permeability, sulphate resistance, and frost-resistance [6, 7].

In cold regions, and particularly for external concrete pavements that are subjected to exposure classes of XD3 and XF4 related to the corrosion and freeze-thaw resistance, extra caution is required to design a durable concrete pavement. These damages can induce some micro and macro cracking in the surface and interior of concrete and subsequently degrade the service life of concrete pavements [8]. Damage resistance concrete technologies developed in recent years, such as self-healing concrete could be a promising solution in reducing the extent of damage or eliminating damage, and subsequently reduce both capital and operational carbon [9]. Self-healing in cement-based materials is generally classified as autogenous and autonomic. The former phenomena represent the self-healing processes that are based on intrinsic properties of the cementitious matrix and dealing with crack width smaller than 150 µm, while the later phenomena deal with larger crack width and it

* Corresponding author: va335@cam.ac.uk

needs the addition of engineered components such as fibres, superabsorbent polymers (SAPs), minerals, capsules, and vascular systems that typically do not exist in the conventional concrete [10].

SAP is a multifunctional material that can be introduced in concrete to adjust the rheology, mitigate plastic and autogenous shrinkage, and enhance the freeze-thaw resistance [11]. SAPs can intake the water and swell depending on their absorption capacity and when they desorb the water inside the concrete, they generate some macro pores that are effective to improve the frost resistance with and without de-icing salts [12]. Mechtcherine et al. [13] conducted an interlaboratory study and investigated the effect of different SAPs on the freeze-thaw resistance of concrete. They reported that SAPs with diameter in the dry state <150 µm is more beneficial than that with particle sizes of up to 300 µm to enhance the freeze-thaw resistance.

The frost resistance of concrete containing different types of SCMs like GGBS at low content was investigated by other researchers [14]. Additionally, the effect of SAPs and fibres on the mechanical and durability properties of concrete was explored in other studies [15, 16]. However, by the knowledge of the author, this is the first study that comprehensively evaluate the freeze-thaw resistance and mass scaling of low carbon RCCs containing 80% GGBS with different smart engineered additives such as SAPs, and Polypropylene (PP) fibres.

2 Experimental programme

2.1 Materials

PC CEM I 52.5N, and Regen GGBS both supplied by Hanson were used as a binder in all concrete mixes. The chemical compositions and physical properties of PC and GGBS that were provided by the producer are listed in Table 1.

Table 1. Chemical and physical properties of binders.

Item	Cementitious materials	
	CEM I 52.5 N	GGBS
SiO_2	19.6	37
Al_2O_3	4.8	13
Fe_2O_3	3.1	0.6
MgO	1.2	8
Na_2O	0.7	0.3
K_2O	0.2	0.6
CaO	64.2	40
	Physical properties	
Density (g/cm^3)	3.16	2.90
Specific surface (m^2/g)	0.30-0.40	0.40-0.50

Sharp sand and gravel with a maximum aggregate size of 2 mm and 11.2 mm were utilized in this study. The sand had a specific gravity of 2.56 and water absorption of 0.6%. The specific gravity and water absorption of gravel were 2.58 and 1.8%, respectively. The sand and gravel were used at the proportions of 45% and 55%, respectively to achieve a uniform aggregate grading. The grading curves of the fine and gravel is shown in Fig. 1. Moreover, a Sikament 700 superplasticiser supplied by Sika Ltd, Hertfordshire, UK was used in concrete mixes as a water reducing admixture to adjust the consistency of concrete mixes. RILEM TC 260-RSC [11] recommended to choose SAP with an absorption behaviour that leads to swollen SAP particles of relatively small sizes to improve freeze-thaw resistance of concrete. Therefore, an irregular particle shapes of a copolymer of acrylamide and acrylate SAPs with particle size 100±21 µm, and a density of ~0.75 g/cm^3 produced by BASF, and 12-mm PP fibres with a density of 0.91 g/cm^3, diameter of 0.03 mm, and aspect ratio of 400 produced by Sika were added in some concrete mixes to explore the effect of smart engineered additives on the properties of RCCs. The optical microscopy image of the SAPs is shown in Fig. 2.

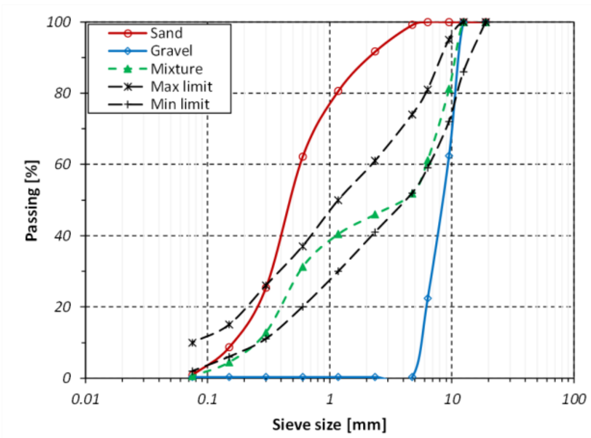

Fig. 1. Aggregates grading curves.

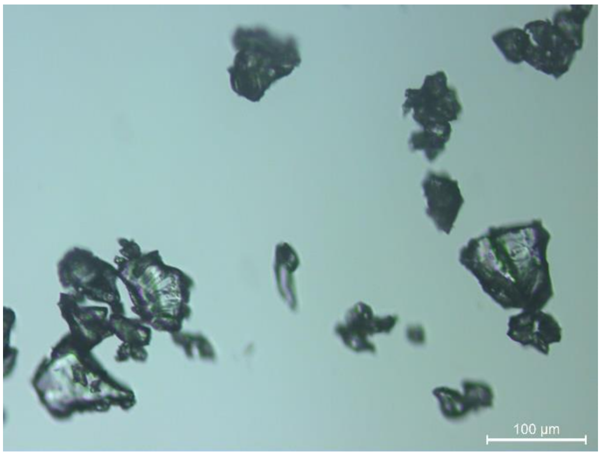

Fig. 2. The optical microscopy image of SAPs.

2.2 Concrete mix design and mixing procedure

In this study four different RCC mixes were developed. The binder of all mixes consisted of 20% PC and 80% of GGBS to develop low carbon concrete mixes and explore the properties of concrete pavements with a high slag content. The first mix was the reference concrete without any additives. The SAPs was added at 0.3% by weight of total binder in the second mix. It should be noted that SAPs was utilised as a dry additive and no additional water was added to the concrete mix to compromise the absorption capacity and swelling properties of SAPs. The absorption capacity of SAPs in the filtrated cement slurry was 20 g/g, which was measured in accordance with the filtration test method described in [17]. The third concrete mix was reinforced with 0.3% by volume fraction of PP fibre. Finally, the fourth concrete mix was produced by combination of both additives of SAPs and PP fibres. All the RCC mixes were developed at water-binder (w/b) ratio of 0.45. The mix proportions of concrete mixes were presented in Table 2. In this table, the dosage of superplasticiser is expressed as a percentage of the total binder mass, and a higher dosage was used for the RCC mixes with self-healing additives.

Table 2. Mix proportion of RCC mixes.

		Mixture ID			
		REF	SAP	PP	SAP-PP
w/b ratio		0.45			
Water	Kg/m^3	126			
CEM I		56			
GGBS		224			
Sand		881			
Gravel		1077			
SAPs	(%)	-	0.3	-	0.3
PP		-	-	0.3	0.3
SP		1.2	1.4	1.4	1.5

The concrete mixing procedure was as follows: first the dry cementitious materials, sand, and SAPs (if applicable) added to the pan mixer and were mixed for 1 minute. Then, the mixing was followed by adding approximately half of the water, which contained the superplasticiser and the mixing continued for another 2 minutes. Finally, the gravel and remaining water were gradually introduced to the mixer and further mixed for 3 minutes. The PP fibres were added gradually to the concrete (if applicable) and mixed for another 5 minutes. By the completion of concrete mixing, the fresh concrete was placed in the cubic steel moulds and plastic cylindrical moulds and compacted by a dynamic vibration hammer to prepare the specimens for the compression and freeze-thaw test. A vibration hammer was used for the compaction of RCC mixes, which was followed by using a vibration table to resemble the field condition that vibratory rollers and/or Pneumatic Tyred Rollers (PTR) are being used. The surface of specimens was covered by a plastic film to avoid the evaporation of the water in the first 24 hours. The concrete specimens were demoulded after 1 day and then immersed in a lime saturated water until their testing ages.

2.3 Testing method

Compression tests were carried out on 100-mm cubic specimens using a 2500-KN universal compression machine in accordance with BS EN 12390-3 at curing ages of 1, 7, 28, and 56 days. Three concrete specimens were prepared and tested for each curing ages.

The freeze-thaw resistance of concrete specimens was determined from the internal structural damage that associated with crack formation and growth by measuring the relative dynamic modulus of elasticity (RDME) as per CEN/TR 15177, while the mass scaling of specimens was measured in accordance with the CEN/TS 12390-9. Three 100×50 mm concrete disk specimens that were obtained by cutting from the 100×200 mm cylindrical specimens were used for the freeze-thaw test, and another three concrete disks with the same dimensions were used for the mass scaling test. The concrete disks were cured in the lime saturated water for the period of 28 days due to the high content of GGBS in mixes. Then, the concrete specimens were sealed in plastic tubes and insulated with polystyrene sheet with 2 cm thickness, while 3 mm deionized water for freeze-thaw test and 3% NaCl solution for mass scaling test were used as a medium on top of the concrete specimens. For the freeze-thaw test, two holes were made in the PVC tubes to fit the transducers and measure the RDME. The specimens then were placed in the freezing chamber and the freeze-thaw cycles were started. The sample preparation and freezing chamber is shown in Fig. 3.

In each 24 hours freeze-thaw cycle, the initial temperature of 20°C was decreased to -4°C within the first 3 hours. Then, the temperature declined to -19°C by twelfth hours, where it was held constant for around 4 hours. The temperature was then gradually raised to reach the temperature of -1°C and 20°C at 19 hours and 24 hours, respectively. The same freeze-thaw cycle was repeated through the completion of the test at 56 cycles. The RDME and weight of scaled materials were measured at each 7 cycles. The RDME was determined by using an ultrasonic pulse transit time (UPTT) measurement device. Two transducers of UPTT device were placed on two opposite sides of the concrete disks so that a constant minimum value was reached, and then the transmission time was measured. The RDME was calculated in percentage as per the Equation (1).

$$RDME = \left(\frac{t_0}{t_n}\right)^2 \times 100\ [\%] \quad (1)$$

Where: RDME is the relative dynamic modulus of elasticity in % determined by using UPTT; t_0 is the initial transit time in μs; and t_n is the transit time measured after n freeze-thaw cycles in μs. The durability factor (DF) of the concrete specimens was also calculated from the RDME according to Equation (2) as per ASTM C666-15 for the evaluation of post-freeze-thaw concrete performance:

$$DF = \frac{RDME.N}{M} \quad (2)$$

Where: RDME is the relative dynamic modulus of elasticity for N freeze-thaw cycles; N the number of freeze-thaw cycles for which the test specimen exhibited the lowest relative dynamic modulus of elasticity; and M the total number of freeze-thaw cycles was conducted (56 cycles in this study). For evaluating the freeze-thaw damage due to de-icing salts, mass scaling was monitored every 7 cycles by filtering and then drying the weight of scaled materials from the surface of concrete specimens as per CEN/TS 12390-9.

Fig. 3. Concrete specimen disks prepared for freeze-thaw and mass scaling tests.

3 Results and discussions

3.1 Compressive strength

The compressive strength test results of different RCC mixes at curing ages of 1, 7, 28, and 56 days is shown in Fig. 4. All the concrete mixes were achieved a strength lower than 4 MPa at 1 day due to the high content of slag used in the mix composition. The CaO content of GGBS is ~38% lower than that of the PC, and this subsequently resulted in a lower hydration and strength development at early ages. Moreover, the superplasticizer added to adjust the consistency of concrete mixes can lead to a retarding effect. It was observed an important strength development in general by increasing the curing age and the average strengths of all concrete specimens at 28 and 56 days were improved by 38% and 51%, respectively compared to that of the 7 days. This can be explained by the higher hydration of the GGBS at later ages of curing that caused a formation of secondary C-S-H gel and densified the microstructure of the cementitious matrix. This result is in agreement with the findings of other researcher who reported concrete mix with high content of slag attained a significant strength improvement at later ages of curing [18].

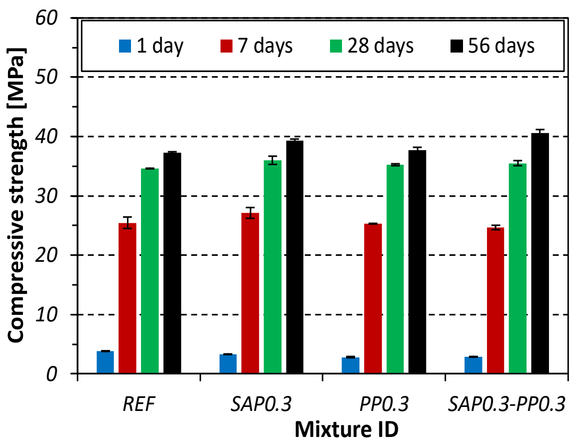

Fig. 4. Compressive strength of different RCC mixes.

The results indicate that the inclusion of smart additives (i.e., PP fibre and SAPs) resulted in a slight improvement in the strength of the self-healing RCC mixes compared to that of the reference mix. For instance, the 56 days strengths of SAP0.3, PP0.3, and SAP0.3-PP0.3 were increased by 5%, 2%, and 9% respectively compared to the REF mix. The addition of PP fibre can restrict the initiation and propagation of microcracks, while the inclusion of SAPs without compensating the water content results in a reduction in w/b ratio due to its absorption capacity, and consequently enhances the compressive strength of self-healing RCC mixes.

3.2 Freeze-thaw resistance

The relative dynamic modulus of elasticity versus the number of freeze-thaw cycles for different RCC mixes is shown in Fig. 5. It was observed that the RDME was gradually decreased up to 21 freeze-thaw cycles, and then followed by an important drop, particularly in case of specimens without fibres (i.e., REF, and SAP0.3 mixes). The continuous freeze-thaw cycles can induce some microcracks into the concrete specimens due to the expansion of frozen water in the pores and propagation of microcracks in matrix can increase the connection between pores and subsequently increasing the permeability properties of concrete that adversely affects the freeze-thaw resistance. The weak frost resistance of concrete rich in GGBS can be attributed to the inadequate development of crystals due to the insufficient formation of calcium hydroxide [7]. Additionally, the inclusion of high content of GGBS in concrete can increase the spacing factor of air voids and lead to an alteration of air void systems, which degrade the freeze-thaw resistance of concrete [19].

The results further indicate that the best performance was achieved in the RCC mix that was reinforced with discrete PP fibres that its freeze-thaw resistance was improved by 28% compared to the reference mix. This can be explained by the bridging ability of fibres to enhance the tensile strength of the matrix and hinder the propagation of microcracks into the concrete [20]. The addition of SAPs in concrete mixes caused an improvement in the RDME of specimens up to 28 cycles and then led to a reduction in the RDME and freeze-thaw resistance of specimens. This can be attributed to the fact that after the internal curing, the SAPs left behind some macropores that are generally in favour of the freeze-thaw resistance. Furthermore, Mechtcherine et al. [11] reported that when no additional water is used to compensate for SAPs absorption, SAPs can intake some of the mixing water, thus leading to reduced w/b ratio, which can decrease the capillary porosity and permeability of concrete and improve freeze–thaw resistance. However, the higher content of air voids in RCC compared to conventional concrete that coupled with additional air voids because of SAPs may adversely affect the frost resistance of RCC specimens. Moreover, it is reported that the positive impact of SAPs on the freeze-thaw resistance of concrete can be potentially reduced if the hydration products fill the air voids produced by SAPs [13]. Additionally, Jones and Weiss [21] stated that the inclusion of SAPs into concrete in the absence of air-entraining admixtures might not be favourable for the freeze-thaw resistance due to the unproper distribution of air voids created by SAPs as well as reabsorbing water that reducing its capability to help upon increment of volume by expansion of water at frozen stage.

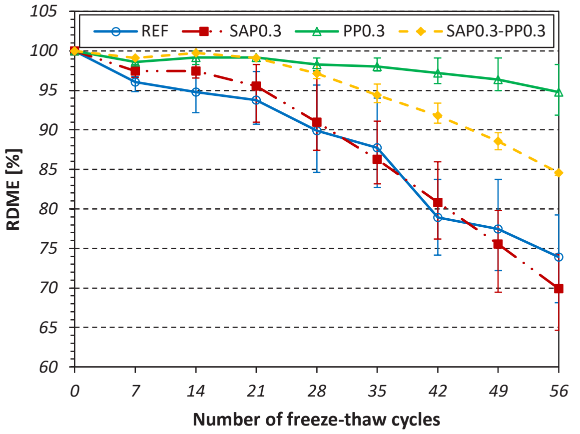

Fig. 5. Relative dynamic modulus of elasticity versus the number of freeze-thaw cycles for different RCC mixes.

The durability factor of different RCC mixes calculated from the Equation (2) and is demonstrated in Fig. 6. Only RCC mixes reinforced with PP fibres had a DF higher than 80%, and classified freeze-thaw resistance as per the classification of ASTM C666-15, while the REF mix and SAP0.3 mix achieved the DF of 73.9%. and 69.9%, respectively. The highest DF was obtained in the RCC mix containing 0.3% PP fibre (i.e., 94.8%) and followed by the self-healing RCC mix containing both PP fibre and SAPs (i.e., 84.6%).

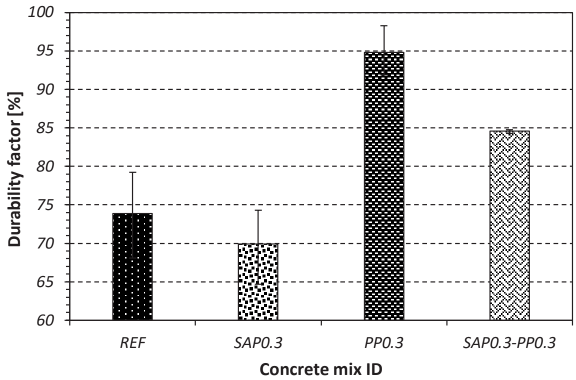

Fig. 6. Durability factor of different RCC mixes.

3.3 Mass scaling

The mass of scaled materials versus the number of freeze-thaw cycles with de-icing salts for different RCC mixes is shown in Fig. 7. Generally, the mass scaling resistance of PC-GGBS blended concrete with high content of GGBS is considered to be lower compared to that of the standard PC concrete [22]. It was reported that the carbonation of concrete manufactured with high content of GGBS causes a change in the microstructure of concrete by coarsening the pore systems, increasing the capillary porosity in the surface layer of concrete and formation of a significant amount of metastable carbonate phases that subsequently result in an inferior frost salt scaling resistance [7, 14, 23]. To ensure sufficient hydration of GGBS in concrete and mitigate the carbonation of RCC mixes rich in GGBS, the water immersion curing in this study was extended to 28 days before subjecting the specimens to freeze-thaw cycles. The results of this study show that weight loss of the REF mix after 7 freeze-thaw cycles (i.e., 0.65 kg/m^2) was almost twice of that of the self-healing RCC mixes (i.e., 0.32 kg/m^2).

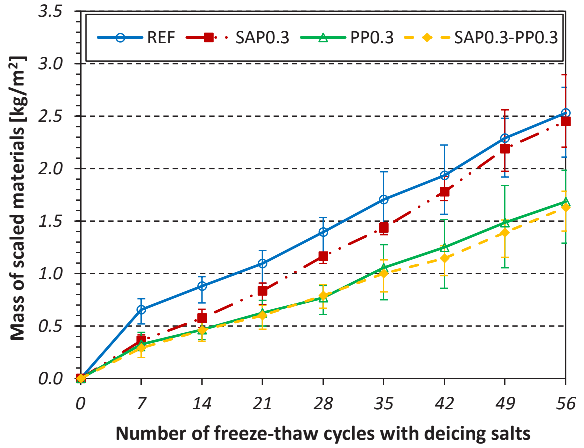

Fig. 7. Mass of scaled materials versus the number of freeze-thaw cycles with de-icing salts for different RCC mixes.

The inclusion of smart engineered additives in the low carbon RCC mixes was effective to mitigate the extent of mass scaling damage. The results further indicate that the effectiveness of PP fibre to improve the frost salt scaling resistance was higher than SAPs. The weight loss of SAP0.3, PP0.3, and SAP0.3-PP0.3 mixes were reduced by 3%, 34%, 36% respectively, compared to that of the REF mix after 56 freeze-thaw cycles. The insignificant influence of SAPs on the mass scaling resistance of concrete could be attributed to the quick desorption of consumed water by SAPs that resulted in an increased capillary pores [24], which might also weaken the ITZ characteristics and subsequently led to an improper frost salt scaling performance. On the other hand, Mechtcherine et al. [11] reported that if SAPs are introduced into concrete without additional water, the frost resistance with de-icing salts can improve remarkably. With respect to the positive effect of fibres on the frost salt scaling resistance of RCCs, the finding of this study is in agreement with the results of other researcher who investigated frost resistance of RCC produced with macro synthetic fibres and concluded that the utilization of fibres enhanced the mass scaling resistance due to the ability of fibres to inhibit the degradation of concrete surface [25].

The results show that none of the RCC mixes developed in this study fulfilled the requirement of the CEN/TS 12390-9 (i.e., maximum mass scaling of 1.0 kg/m^2 after 56 freeze-thaw cycles) to be considered a frost salt scaling resistance concrete. The weight loss of REF, SAP0.3, PP0.3, and SAP0.3-PP0.3 mixes after 56 freeze-thaw cycled were 2.53, 2.45, 1.68, and 1.63 kg/m^2 respectively. Fig. 8 shows the surface damage of concrete specimens exposed to 3% NaCl after 56 freeze-thaw cycles. The extent of damage was reduced in self-healing RCC specimens containing fibres, and the deterioration was mainly due to the paste degradation, while in REF mix and SAP0.3 mix, the extent of damage raised from the cement paste to detachment of coarse aggregates.

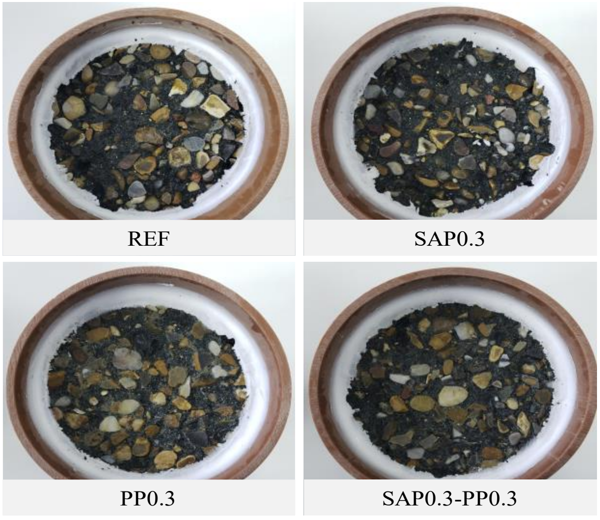

Fig. 8. Appearance the surface damage of different RCC exposed to de-icing salts after 56 freeze-thaw cycles.

4 Conclusions

This paper explored the compressive strength and freeze-thaw resistance of low carbon self-healing RCC pavements. From the experimental test results, the following conclusions can be drawn:

1) The RCC mixes containing 80% GGBS and 20% PC achieved a compressive strength of around 40 MPa at 56 days. The inclusion of PP fibres and SAPs resulted in an improvement in the strength of concrete.
2) The addition of SAPs had insignificant influence on the freeze-thaw resistance of concrete. The best performance was achieved in the mixes reinforced with 0.3% PP fibres.
3) Only concrete specimens reinforced with PP fibres classified as freeze-thaw resistance and obtained a durability factor of greater than 80%.
4) The addition of SAPs into concrete slightly improved the mass scaling resistance, while the combination of SAPs and PP fibres into low carbon RCCs mitigated the frost salts degradation and led to a significant reduction in the weight loss of specimens exposed to de-icing salts.

This project has received funding from the European Union's Horizon 2020 research and innovation programme under the Marie Skłodowska-Curie grant agreement No 101034337.

References

1. D. Dey, D. Srinivas, B. Panda, P. Suraneni, T.G. Sitharam, J. Clea. Pro. 130749, (2022)
2. A. Alsaif, R. Garcia, F.P. Figueiredo, K. Neocleous, A. Christofe, M. Guadagnini, K. Pilakoutas, Eng. Stru. **193**, 170-183, (2019)
3. E. Sheikh, S.R. Mousavi, I. Afshoon, J. Clea. Pro. **368**, 133005, (2022)
4. E. Gartner, H. Hirao, Cem. Con. Res. **78**, 126-142, (2015)
5. M. Amran, G. Murali, N.H.A. Khalid, R. Fediuk, T. Ozbakkaloglu, Y.H. Lee, ... & Y.Y. Lee, Con. Buil. Mat. **272**, 121942, (2021)
6. M.C. Juenger, R. Siddique, Cem. Con. Res. **78**, 71-80, (2015)
7. R. Wang, Z. Hu, Y. Li, K. Wang, H. Zhang, Con. Buil. Mat. **321**, 126371, (2022)
8. S. Luo, T. Bai, M. Guo, Y. Wei, W. Ma, Mat. **15**(13), 4568, (2022)
9. N. De Belie, E. Gruyaert, A. Al-Tabbaa, P. Antonaci, C. Baera, D. Bajare, ... & H.M. Jonkers, Adv. Mat. Inter. **5**(17), 1800074, (2018)
10. A. Al-Tabbaa, C. Litina, P. Giannaros, A. Kanellopoulos, L. Souza, Con. Buil. Mat. **208**, 669-685, (2019)
11. V. Mechtcherine, C. Schröfl, M. Reichardt, A.J. Klemm, K.H. Khayat, Mat. Stru. **52**, 1-7, (2019)
12. C. Schröfl, K.A. Erk, W. Siriwatwechakul, M. Wyrzykowski, D. Snoeck, Cem. Con. Res. **151**, 106648, (2022)
13. V. Mechtcherine, C. Schröfl, M. Wyrzykowski, M. Gorges, P. Lura, D. Cusson, ... & J. Weiss, Mat. Stru. **50**(1), 1-19, (2017)
14. V. Correia, J. Gomes Ferreira, L. Tang, A. Lindvall, Appl. Sci. **10**(11), 3940, (2020)
15. V. Mechtcherine, M. Wyrzykowski, C. Schröfl, D. Snoeck, P. Lura, N. De Belie, ... & S.I. Igarashi, Mat. Stru. **54**(2), 1-20, (2021)
16. D. Snoeck, K. Van Tittelboom, S. Steuperaert, P. Dubruel, & N. De Belie, J. Intel. Mat. Syst. and Stru. **25**(1), 13-24, (2014)
17. M.M. Zohourian, & K. Kabiri, Iran. Poly. J. **17**(6), 451–447, (2008)
18. A. Gholampour, & T. Ozbakkaloglu, J. Clea. Pro. **162**, 1407-1417, (2017)
19. Z. Giergiczny, M.A. Glinicki, M. Sokołowski, & M. Zielinski, Con. Buil. Mat. **23**(6), 2451-2456, (2009)
20. J. Ren, & Y. Lai, Col. Reg. Sci. Tech. **188**, 103301, (2021)
21. W.A. Jones, & W.J. Weiss, 4th Int. Conference on the Durability of Concrete Structures, 24–26 July 2014, Purdue University, USA, (2014)
22. J. Stark, & H.M. Ludwig, Mat. J. **94**(1), 47-55, (1997)
23. O. Copuroglu, The characterisation, improvement and modelling aspects of frost salt scaling of cement-based materials with a high slag content, PhD Thesis, Tu Delft, (2006)
24. M. Kim, S.H. Kang, S.G. Hong, & J. Moon, Mat. **12**(23), 3863, (2019)
25. Z. Algin, & S. Gerginci, Con. Buil. Mat. **234**, 117382, (2020)